J|A|C|S
ARTICLES
Published on Web 01/07/2004

Influences of Ribonucleotide on a Duplex Conformation and Its Thermal Stability: Study with the Chimeric RNA−DNA Strands

Shu-ichi Nakano,[†] Takayuki Kanzaki,[‡] and Naoki Sugimoto*[,†,†,§]

Contribution from the High Technology Research Center, Department of Chemistry, Faculty of Science and Engineering, and Frontier Institute for Biomolecular Engineering Research (FIBER), Konan University, 8-9-1 Okamoto, Higashinada-ku, Kobe, 658-8501, Japan

Received July 16, 2003; E-mail: sugimoto@konan-u.ac.jp

Abstract: To understand the influences of the ribonucleotide on a duplex conformation and its stability, we systematically studied the CD spectra and the thermodynamics of nucleic acid duplexes formed by the chimeric RNA−DNA strand in which ribonucleotides and deoxyribonucleotides were covalently attached. It was found that the duplex stability was context-dependent and independent of the number of ribonucleotides in the chimeric strand, whereas the CD spectra showed less overall structural perturbation by the chimeric junctions. Combining the results of the CD and the thermodynamic data revealed a stability−structure relationship for the duplexes. Importantly, $\Delta G°_{37}$ values estimated for the chimeric junction formation in the RNA−DNA/DNA and the RNA−DNA/RNA duplexes were close to those of RNA/DNA and RNA/RNA interactions, respectively. Furthermore, $\Delta G°_{37}$s of the DNA−RNA/DNA and DNA−RNA/DNA−RNA junctions were similar to those of the DNA duplex, and the values of DNA−RNA/RNA−DNA were similar to those of the DNA/RNA. The thermodynamic analyses suggest that the 5′-nucleotide may be the crucial factor that determines the stability at the chimeric junction. Our results not only suggest influences of the ribonucleotide on a duplex conformation and its stability but also are useful for the design of RNA−DNA chimeric strands applicable to biotechnology.

Introduction

The physical properties of RNA and DNA, such as their helical conformation, structural polymorphism, and protein binding differ substantially despite the similarity in the chemical structure of their Watson−Crick base pairs. These differences originated from the 2′ group of the sugar moiety, for example, the 2′-hydroxyl group of the ribonucleotide affects the sugar puckering preferring the C3′-*endo* mode and interactions via the 2′-hydroxyl group are often found in tertiary structures of the RNA itself and the RNA-protein complex.[1] The quantitative investigation of the 2′-hydroxyl group of the ribonucleotide is one of the important issues to be addressed.

Typical RNA duplex and a DNA one form a different helical conformation, A- and B-form, respectively. The thermal stability of an RNA duplex is generally greater than that of a DNA duplex when their sequences are identical.[2] Most RNA/DNA hybrid duplexes adopt an A-like conformation, however, the thermal stability of an RNA/DNA duplex is substantially lower than the RNA duplex with the same sequence,[2a,3] indicating that the helical conformation may not be the major factor that determines the duplex stability.

The chimeric strand of RNA−DNA carries a junction covalently linking an upstream ribonucleotide and a downstream deoxyribonucleotide as depicted in Figure 1A. Replication of the lagging strand requires an RNA−DNA strand paired with a DNA (RNA−DNA/DNA duplex).[4] Another type of chimeric duplex seen in biological systems is the RNA−DNA/RNA formed by an RNA−DNA strand and a genomic RNA during reverse transcription of viral RNAs.[5] Recently, chimeric nucleotides have been evaluated for applicability in gene targeting,[6] as gene repair materials,[7] PCR primers,[8] and sequence-specific mediators of RNA interference (RNAi),[9] which use the DNA−RNA strands as well as the RNA−DNA ones (Figure 1A).

Here, we systematically investigated the influences of the ribonucleotide on a duplex conformation and the thermal stability using the chimeric strands of RNA−DNA and DNA−

[†] High Technology Research Center.
[‡] Department of Chemistry, Faculty of Science and Engineering.
[§] Frontier Institute for Biomolecular Engineering Research (FIBER).
* Corresponding author.

(1) Bloomfield, V. A.; Crothers, D. M.; Tinoco, I., Jr. *NUCLEIC ACIDS*; University Science Books: CA, 2000.
(2) (a) Riley, M.; Maling, B.; Chamberlin, M. J. *J. Mol. Biol.* **1966**, *20*, 359. (b) Krakauer, H.; Sturtevant, J. M. *Biopolymers* **1968**, *6*, 491. (c) Scheffler, I. E.; Sturtevant, J. M. *J. Mol. Biol.* **1969**, *42*, 577. (d) Borer, P. N.; Dengler, B.; Tinoco, I., Jr.; Uhlenbeck, O. C. *J. Mol. Biol.* **1974**, *86*, 843. (e) Breslauer, K. J.; Sturtevant, J. M.; Tinoco, I., Jr. *J. Mol. Biol.* **1975**, *99*, 549. (f) Wang, S.; Kool, E. T. *Biochemistry* **1995**, *34*, 4125.
(3) Sugimoto, N.; Nakano, S.; Katoh, M.; Matsumura, A.; Nakamuta, H.; Ohmichi, T.; Yoneyama, M.; Sasaki, M. *Biochemistry* **1995**, *34*, 11 211.
(4) Ogawa, T.; Okazaki, T. *Annu. Rev. Biochem.* **1980**, *49*, 421.
(5) Gotte, M.; Li, X.; Wainberg, M. A. *Arch. Biochem. Biophys.* **1999**, *365*, 199.
(6) Shimayama, T.; Nishikawa, F.; Nishikawa, S.; Taira, K. *Nucleic Acids Res.* **1993**, *21*, 2605.
(7) (a) Rice, M. C.; Czymmek, K.; Kmiec, E. B. *Nat. Biotechnol.* **2001**, *19*, 321. (b) Gamper, H. B.; Parekh, H.; Rice, M. C.; Bruner, M.; Youkey, H.; Kmiec, E. B. *Nucleic Acids Res.* **2000**, *28*, 4332.
(8) Coljee, V. W.; Murray, H. L.; Donahue, W. F.; Jarrell, K. A. *Nat. Biotechnol.* **2000**, *18*, 789.
(9) Elbashir, S. M.; Harborth, J.; Lendeckel, W.; Yalcin, A.; Weber, K.; Tuschl, T. *Nature* **2001**, *411*, 494.

10.1021/ja037314h CCC: $27.50

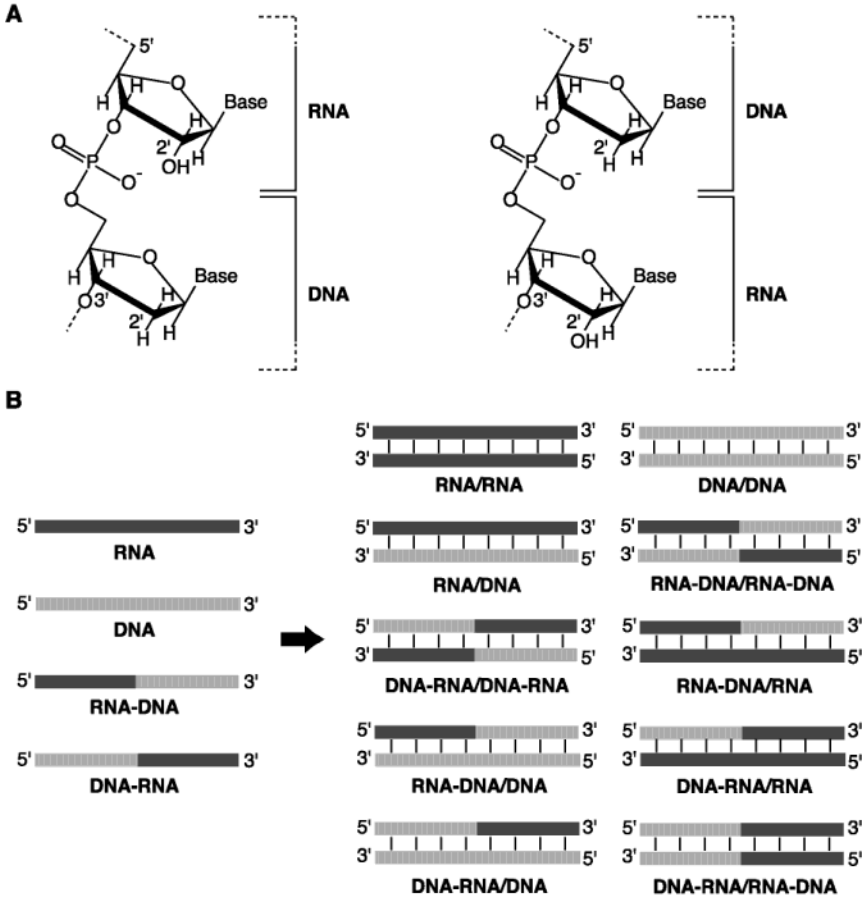

Figure 1. (A) Chemical structures for the chimeric RNA-DNA (left) and chimeric DNA−RNA strand (right). (B) Duplexes formed by four kinds of nucleotides of RNA, DNA, RNA−DNA, and DNA−RNA strand.

RNA. We designed 26 nonself-complementary chimeric duplexes and 4 normal duplexes (one RNA duplex, one DNA duplex, and two RNA/DNA hybrid duplexes) as a control, and their CD (circular dichroism) spectra and melting profiles were measured. It is demonstrated that the thermodynamic contributions from the chimeric junctions are close either to those from DNA/DNA, RNA/RNA, or RNA/DNA interactions depending on the 5′-nucleotide at the junction. Our results suggest that the nearest-neighbor interaction may involve a contribution of the 2′-hydroxyl group as well as the hydrogen bonds in base pairing and stacking interactions between adjacent base pairs and that the 2′-hydroxyl group in the ribonucleotide confers a greater stability on the RNA duplexes.

Materials and Methods

Preparation of the Oligonucloeotides. The synthesis and purification of the chimeric RNA−DNA and DNA−RNA strands were the same as those reported for the RNA oligomer syntheses.[10] We chemically synthesized 18 nonself-complementary chimeric strands, and RNA and DNA strands (Tables 1−3) on a solid support using the phosphoramidite chemistry. All nucleotides containing any ribonucleotide were prepared by a trityl-off variation. All of the nucleotides were purified with reversed-phase HPLC (high-performance liquid chromatography) after deprotection of the protecting groups, followed by desalting with a C-18 Sep-Pak cartridge column.

(10) Kierzek, R.; Caruthers, M. H.; Longfellow, C. E.; Swinton, D.; Turner, D. H.; Freier, S. M. *Biochemistry* **1986**, *25*, 7840.

Measurement of the CD Spectra. The CD spectra were obtained using a JASCO J-600 or J-820 spectropolarimeter equipped with a temperature controller. The CD spectra were measured from 200 to 320 nm in a 0.1 cm path length cuvette. The total concentration of the strands was 70 μM. All spectra were measured at 5 °C in a buffer containing 1 M NaCl, 10 mM Na_2HPO_4, and 1 mM Na_2EDTA at pH 7.0.

Measurement and Analysis of the Melting Profiles. The UV absorbance was measured with a Hitachi U-3200, U-3210, or Shimazu 1650 spectrophotometer equipped with a temperature controller. The melting curves (absorbance vs temperature curves) were monitored at 260 nm at a heating rate of 0.5 or 1.0 °C/min in a buffer containing 1 M NaCl, 10 mM Na_2HPO_4, and 1 mM Na_2EDTA at pH 7.0, which is the condition at which the nearest-neighbor parameters for RNA/RNA, DNA/DNA, and RNA/DNA were determined.[3,11]

The thermodynamic parameters ($\Delta H°$, $\Delta S°$, and $\Delta G°$ at 37 °C) were calculated from the melting temperature (T_m) values at different total strand concentrations (C_ts) (T_m^{-1} vs $\log(C_t/4)$ plot),[2d,12] and their standard deviations were obtained, as

(11) (a) Breslauer, K. J.; Frank, R.; Blocker, H.; Marky, L. A. *Proc. Natl. Acad. Sci. U.S.A.* **1986**, *83*, 3746. (b) Freier, S. M.; Kierzek, R.; Jaeger, J. A.; Sugimoto, N.; Caruthers, M. H.; Neilson, T.; Turner, D. H. *Proc. Natl. Acad. Sci. U.S.A.* **1986**, *83*, 9373. (c) Turner, D. H.; Sugimoto, N.; Freier, S. M. *Annu. Rev. Biophys. Biophys. Chem.* **1988**, *17*, 167. (d) Jaeger, J. A.; Turner, D. H.; Zuker, M. *Proc. Natl. Acad. Sci. U.S.A.* **1989**, *86*, 7706. (e) Sugimoto, N.; Nakano, S.; Yoneyama, M.; Honda, K. *Nucleic Acids Res.* **1996**, *24*, 4501. (f) SantaLucia, J., Jr. *Proc. Natl. Acad. Sci. U.S.A.* **1998**, *95*, 1460. (g) Xia, T.; SantaLucia, J., Jr.; Burkard, M. E.; Kierzek, R.; Schroeder, S. J.; Jiao, X.; Cox, C.; Turner, D. H. *Biochemistry* **1998**, *37*, 14719.

Table 1. Thermodynamic Parameters for the Duplex Formations Involving the RNA−DNA Strand[a]

sequence[b]	abbreviation	$\Delta H°$ (kcal mol^{-1})	$\Delta S°$ (cal mol^{-1} K^{-1})	$\Delta G°_{37}$ (kcal mol^{-1})	T_m (°C)
		RNA−DNA/RNA			
r(GACUAGG)d(T)/r(ACCUAGUC)	**r7d1/r8**	−70.1 (−69.2)	−190 (−189)	−11.2 (−10.5)	59.2 (54.9)
r(GACUAG)d(GT)/r(ACCUAGUC)	**r6d2/r8**	−67.6 (−64.9)	−183 (−176)	−10.8 (−10.5)	58.1 (57.0)
r(GACUA)d(GGT)/r(ACCUAGUC)	**r5d3/r8**	−70.7 (−62.0)	−197 (−169)	−9.75 (−9.7)	51.8 (53.1)
r(GACU)d(AGGT)/r(ACCUAGUC)	**r4d4/r8**	−66.7 (−61.4)	−186 (−170)	−9.19 (−8.9)	49.9 (49.1)
r(GAC)d(TAGGT)/r(ACCUAGUC)	**r3d5/r8**	−64.1 (−61.1)	−179 (−170)	−8.68 (−8.4)	47.7 (46.5)
r(GA)d(CTAGGT)/r(ACCUAGUC)	**r2d6/r8**	−66.2 (−62.6)	−186 (−174)	−8.55 (−8.5)	46.8 (47.1)
r(G)d(ACTAGGT)/r(ACCUAGUC)	**r1d7/r8**	−64.3 (−60.2)	−182 (−167)	−7.89 (−7.5)	43.7 (42.3)
		RNA−DNA/DNA			
r(GACUAGG)d(T)/d(ACCTAGTC)	**r7d1/d8**	−66.5 (−55.3)	−188 (−155)	−8.34 (−7.3)	45.7 (41.5)
r(GACUAG)d(GT)/d(ACCTAGTC)	**r6d2/d8**	−65.4 (−56.9)	−187 (−159)	−7.37 (−7.7)	41.0 (43.6)
r(GACUA)d(GGT)/d(ACCTAGTC)	**r5d3/d8**	−68.2 (−55.0)	−197 (−155)	−7.31 (−6.9)	40.6 (39.1)
r(GACU)d(AGGT)/d(ACCTAGTC)	**r4d4/d8**	−68.8 (−52.5)	−201 (−148)	−6.69 (−6.6)	37.7 (37.4)
r(GAC)d(TAGGT)/d(ACCTAGTC)	**r3d5/d8**	−63.3 (−51.3)	−182 (−143)	−6.90 (−6.9)	38.8 (39.2)
r(GA)d(CTAGGT)/d(ACCTAGTC)	**r2d6/d8**	−60.0 (−50.9)	−170 (−140)	−7.30 (−7.5)	41.0 (43.1)
r(G)d(ACTAGGT)/d(ACCTAGTC)	**r1d7/d8**	−63.0 (−54.4)	−181 (−153)	−6.84 (−6.9)	38.5 (39.2)
		RNA/RNA			
r(GACUAGGU)/r(ACCUAGUC)	**r8/r8**	−69.0 (−69.2)	−186 (−189)	−11.3 (−10.5)	60.0 (55.7)
		DNA/DNA			
d(GACTAGGT)/d(ACCTAGTC)[c]	**d8/d8**	−65.6 (−57.7)	−191 (−163)	−6.5 (−7.1)	37.2 (40.2)
		RNA/DNA			
r(GACUAGGU)/d(ACCTAGTC)[d]	**r8/d8**	−57.0 (−54.0)	−158 (−150)	−8.1 (−7.6)	43.3 (43.3)
		DNA/RNA			
d(GACTAGGT)/r(ACCUAGUC)[d]	**d8/r8**	−56.0 (−53.6)	−159 (−150)	−6.9 (−7.0)	39.2 (39.6)

[a] Measurements were conducted in a buffer containing 1 M NaCl, 10 mM Na_2HPO_4, and 1 mM Na_2EDTA (pH 7.0). The thermodynamic parameters were determined from T_m^{-1} vs $\log(C_t/4)$ plots and curve fitting methods. T_m is the melting temperature at 100 μM total strand concentration. The average errors for $\Delta H°$, $\Delta S°$, and $\Delta G°_{37}$ in Tables 1−3 are 3.3%, 3.6%, and 2.8%, respectively. Values in the parentheses are the prediction values as described in the text. [b] The strand orientates 5′ → 3′ from left to right, and r and d indicate ribonucleotide and deoxyribonucleotide, respectively. The slash separates the strand sequences. [c] Data from Sugimoto et al.[11e] [d] Data from Sugimoto et al.[3]

Table 2. Thermodynamic Parameters for the Duplex Formations Involving the DNA−RNA Strand[a]

sequence	abbreviation	$\Delta H°$ (kcal mol^{-1})	$\Delta S°$ (cal mol^{-1} K^{-1})	$\Delta G°_{37}$ (kcal mol^{-1})	T_m (°C)
		DNA−RNA/RNA			
d(GACTA)r(GGU)/r(ACCUAGUC)	**d5r3/r8**	−67.8 (−62.1)	−191 (−176)	−8.58 (−7.5)	46.7 (42.3)
d(GACT)r(AGGU)/r(ACCUAGUC)	**d4r4/r8**	−67.7 (−62.7)	−188 (−175)	−9.41 (−8.3)	50.9 (46.2)
d(GAC)r(UAGGU)/r(ACCUAGUC)	**d3r5/r8**	−72.1 (−63.0)	−200 (−175)	−10.2 (−8.8)	53.4 (48.7)
		DNA−RNA/DNA			
d(GACTA)r(GGU)/d(ACCTAGTC)	**d5r3/d8**	−56.7 (−58.0)	−159 (−163)	−7.34 (−7.5)	41.5 (42.5)
d(GACT)r(AGGU)/d(ACCTAGTC)	**d4r4/d8**	−61.7 (−60.5)	−175 (−169)	−7.56 (−7.8)	42.3 (43.8)
d(GAC)r(UAGGU)/d(ACCTAGTC)	**d3r5/d8**	−57.8 (−61.7)	−161 (−175)	−7.83 (−7.5)	44.2 (42.2)

[a] See the footnotes in Table 1.

Table 3. Thermodynamic Parameters for the Duplex Formations of the Two Chimeric Strands[a]

sequence	abbreviation	$\Delta H°$ (kcal mol^{-1})	$\Delta S°$ (cal mol^{-1} K^{-1})	$\Delta G°_{37}$ (kcal mol^{-1})	T_m (°C)
		DNA−RNA/RNA−DNA			
d(GACTA)r(GGU)/r(ACC)d(TAGTC)	**d5r3/r3d5**	−56.6 (−60.2)	−158 (−168)	−7.67 (−8.0)	43.3 (44.9)
d(GACT)r(AGGU)/r(ACCU)d(AGTC)	**d4r4/r4d4**	−59.8 (−62.0)	−166 (−173)	−8.40 (−8.4)	47.1 (46.8)
		DNA−RNA/DNA−RNA			
d(GACTA)r(GGU)/d(ACC)r(UAGUC)	**d5r3/d3r5**	−66.7 (−59.9)	−192 (−170)	−7.25 (−7.1)	40.4 (40.2)
d(GACT)r(AGGU)/d(ACCT)r(AGUC)	**d4r4/d4r4**	−60.2 (−61.2)	−169 (−172)	−7.69 (−7.7)	43.1 (43.2)
		RNA−DNA/RNA−DNA			
r(GACUA)d(GGT)/r(ACC)d(TAGTC)	**r5d3/r3d5**	−70.5 (−48.4)	−201 (−132)	−8.17 (−7.3)	44.4 (42.2)
r(GACU)d(AGGT)/r(ACCU)d(AGTC)	**r4d4/r4d4**	−63.2 (−48.1)	−178 (−132)	−8.03 (−7.1)	44.6 (40.5)

[a] See the footnotes in Table 1.

reported.[13] Additionally, the melting curves were fit with a theoretical equation to obtain the thermodynamic parameters.[12] The thermodynamic parameters used for the comparisons were the averages obtained from the T_m^{-1} vs $\log(C_t/4)$ plot and the curve fittings.

Calculation of the Energy for the Base Pairing at the Chimeric Junction. The $\Delta G°_{37}$ values for the formation of the chimeric junction were calculated based on the nearest-neighbor model that has been proven to be applicable to most oligonucleotide duplexes.[3,11] The nearest-neighbor $\Delta G°_{37}$s at the chimeric junctions (denoted rd/rr, rd/dd, dr/rr, dr/dd, dr/rd, dr/dr, and rd/rd for RNA−DNA/RNA, RNA−DNA/DNA, DNA−RNA/RNA, DNA−RNA/DNA, DNA−RNA/RNA−DNA, DNA−RNA/DNA−RNA, and RNA−DNA/RNA−DNA, respectively) were calculated by subtracting the nearest-neighbor free energies of the RNA/RNA (rr/rr), DNA/DNA (dd/dd), and RNA/DNA (rr/dd and dd/rr) interactions in a duplex from observed $\Delta G°_{37}$ ($\Delta G°_{37,obs}$).[11c,d] We used 3.4 kcal mol^{-1} theoretically determined as the initiation factor[1,11a−c] in order to compare the parameters of the chimeric junctions with those of the RNA/RNA, DNA/DNA, RNA/DNA, and DNA/RNA. For example, the $\Delta G°_{37}$ for

(12) (a) Marky, L. A.; Breslauer, K. J. *Biopolymers* **1987**, *26*, 1601. (b) Puglish, J. D.; Tinoco, I., Jr. *Methods Enzymol.* **1989**, *180*, 304.
(13) Bevington, P. R. *Data Reduction and Error Analysis for the Physical Sciences*; McGraw-Hill: New York, 1969.

rUdA/rUA in the r(GACU)d(AGGT)/r(ACCUAGUC) duplex was calculated by the following equation.

$$\Delta G^\circ_{37}(\text{rUdA/rUA}) = \Delta G^\circ_{37,\text{obs}} - \{\Delta G^\circ_{37}(\text{rGA/rUC}) + \Delta G^\circ_{37}(\text{rAC/rGU}) + \Delta G^\circ_{37}(\text{rCU/rAG}) + \Delta G^\circ_{37}(\text{dAG/rCU}) + \Delta G^\circ_{37}(\text{dGG/rCC}) + \Delta G^\circ_{37}(\text{dGT/rAC})\} - 3.4 \text{ (kcal/mol)}$$

Results and Discussion

Design of the Sequences of the Chimeric Strand. Figure 1B shows 10 types of duplexes formed by RNA, DNA, RNA−DNA, and DNA−RNA strands. The chimeric strands were designed based on 5′-GACUAGGU-3′ or 5′-ACCUAGUC-3′ by replacing ribonucleotides with deoxyribonucleotides from the 3′ or 5′ end. For comparison, measurements of an RNA duplex of r(GACUAGGU)/r(ACCUAGUC) (**r8/r8**), a DNA duplex of d(GACTAGGT)/d(ACCTAGTC) (**d8/d8**), and two RNA/DNA hybrid duplexes of r(GACUAGGU)/d(ACCTAGTC) (**r8/d8**) and d(GACTAGGT)/r(ACCUAGUC) (**d8/r8**) were also performed. The **r8/r8** is responsible for a nondeoxyribonucleotide type of the RNA−DNA/RNA and DNA−RNA/RNA duplexes, and **d8/r8** is a nonribonucleotide type of these chimeric duplexes. Similarity, **r8/d8** and **d8/d8** are responsible for the nondeoxyribonucleotide and nonribonucleotide types of the RNA−DNA/DNA and DNA−RNA/DNA duplexes, respectively.

Effect of the Chimeric Junction on the Duplex Conformation. Generally, an A-form duplex shows an intense positive peak around 270 nm, a small negative peak around 235 nm, and a large negative band at 210 nm, whereas a B-form duplex reveals moderate bands at 280 and 240 nm. Figure 2 compares the CD spectra of the chimeric duplexes with those of the control duplexes (see the sequences and their abbreviations in Tables 1−3). Because all of the duplexes have an identical sequence except for thymine in deoxyribonucleotide in place of uridine in ribonucleotide, the difference in the spectra mostly originated from the difference in the conformation.[14] The CD spectra of **r8/r8** and **d8/d8** were representative of A- and B-forms, respectively, and those of the hybrid duplexes (**r8/d8** and **d8/r8**) were similar to the A-form spectrum of **r8/r8**.

All of the RNA−DNA/RNA duplexes exhibited a spectrum similar to **r8/r8** or **d8/r8** (Figure 2A), whereas the RNA−DNA/DNA duplexes showed a spectrum intermediate between **r8/d8** and **d8/d8** (Figure 2B). The band intensity around 270 nm did not change systematically with the number of ribonucleotides in the chimeric strand. The spectra of the DNA−RNA paired with the RNA were representative of an A-form (Figure 2C), and those of the DNA−RNA paired with the DNA were intermediate between **r8/d8** and **d8/d8** (Figure 2D). All of the duplexes formed by the two chimeric strands (DNA−RNA/RNA−DNA, DNA−RNA/DNA−RNA, or RNA−DNA/RNA−DNA) showed an A-like spectrum (Figure 2E−G), and there is no significant structural perturbation by the chimeric junction that might affect the CD spectrum.

The large negative band at 210 nm characteristic of an A-form helix is used for estimation of a conformational fraction of RNA/DNA duplexes in comparison with the RNA duplex and the DNA duplex spectra with the same sequence.[15] A large positive band around 265 nm is also characteristic of an A-form duplex, although the relevance of these CD bands remains unclear. Figure 3A shows a linearity of the CD intensities between at 210 nm and at 265 nm. The duplexes in Figure 2 have an identical sequence, so that the difference in the CD bands mostly originated from the duplex conformation without the influence of the sequence. The linearity in Figure 3A indicates that both CD bands reflect the helical conformation, and it is proposed that the conformation of the chimeric duplexes may continuously vary between the A- and B-forms as suggested for the RNA/DNA hybrid duplex[15] since a CD spectrum reflects all possible structures in solution both thermodynamically and kinetically in a rapid equilibrium.

Thermal Stability of the Duplexes Containing the Chimeric Strand. Melting profiles of the duplexes measured in a buffer containing 1 M NaCl, 10 mM Na_2HPO_4, and 1 mM Na_2-EDTA (pH 7.0) revealed that all the duplexes examined here exhibited a good agreement for the ΔH° and ΔS° values determined from the T_m^{-1} vs $\log(C_t/4)$ plot and the curve fitting methods, suggesting a two-state transition.[12b] Table 1 summarizes the thermodynamic parameters of the RNA−DNA/RNA and the RNA−DNA/DNA duplexes compared with those of the control duplexes. In the normal duplexes, **r8/r8** was the most stable ($\Delta G^\circ_{37} = -11.3$ kcal mol^{-1}) and **d8/d8** was the least (-6.5 kcal mol^{-1}). The stability of the hybrid duplexes, **r8/d8** and **d8/r8**, was -8.1 and -6.9 kcal mol^{-1}, respectively, which were intermediate between those of **r8/r8** and **d8/d8**, but not the average of the two.

The values of ΔG°_{37} for the RNA−DNA/RNA duplexes ranged from -11.2 to -7.89 kcal mol^{-1}, which was intermediate between those of **r8/r8** and **d8/r8**, and the stability increased with the number of ribonucleotides in the chimeric strand. The RNA−DNA/DNA duplexes showed $-8.34 \sim -6.69$ kcal mol^{-1} in ΔG°_{37} that indicated less stability than that of the RNA−DNA/RNA duplexes. However, decreasing the number of ribonucleotides did not systematically decrease the stability of the RNA−DNA/DNA duplex, for example, removal of the single 2′-hydroxyl group from **r3d5/d8** increased the stability by 0.40 kcal mol^{-1}. Similar observation is reported for triplexes that the replacement of deoxyribothymidine to ribouridine in the third strand affects the stability (stabilization or destabilization) depending on the position of the replacement.[16] Qualitatively, the intensity of the positive CD band at 265 nm in Figure 2B is relevant to the duplex stability; the order of intensity is **r7d1/d8** ≫ **r5d3/d8** > **r2d6/d8** > **r6d2/d8** ∼ **r1d7/d8** ∼ **r3d5/d8** ∼ **r4d4/d8**, and the order of the thermal stability is **r7d1/d8** ≫ **r5d3/d8** ∼ **r2d6/d8** ∼ **r6d2/d8** > **r1d7/d8** ∼ **r3d5/d8** ∼ **r4d4/d8**.

Table 2 summarizes the thermodynamic parameters of the DNA−RNA/RNA and DNA−RNA/DNA duplexes. Their thermal stability demonstrates the same trend as seen in Table 1, in which the chimeric strand paired with RNA is more stable than that paired with DNA. Tables 1 and 2 indicate that decreasing the number of ribonucleotides in the chimeric strand systematically decreases the duplex stability of the RNA−DNA or DNA−RNA strand associated with RNA, but not for the chimeric strands associated with DNA. This would originate

(14) Because the CD spectra reported for uridine and thymine are almost identical [Sprecher, C. A.; Johnson, W. C., Jr. *Biopolymers* **1977**, *16*, 2243.], it is unlikely that the substitution of U with T changed the CD spectra.

(15) Lesnik, E. A.; Freier, S. M. *Biochemistry* **1995**, *34*, 10 807.
(16) Bernal-Mendez, E.; Leumann, C. J. *Biochemistry* **2002**, *41*, 12 343.

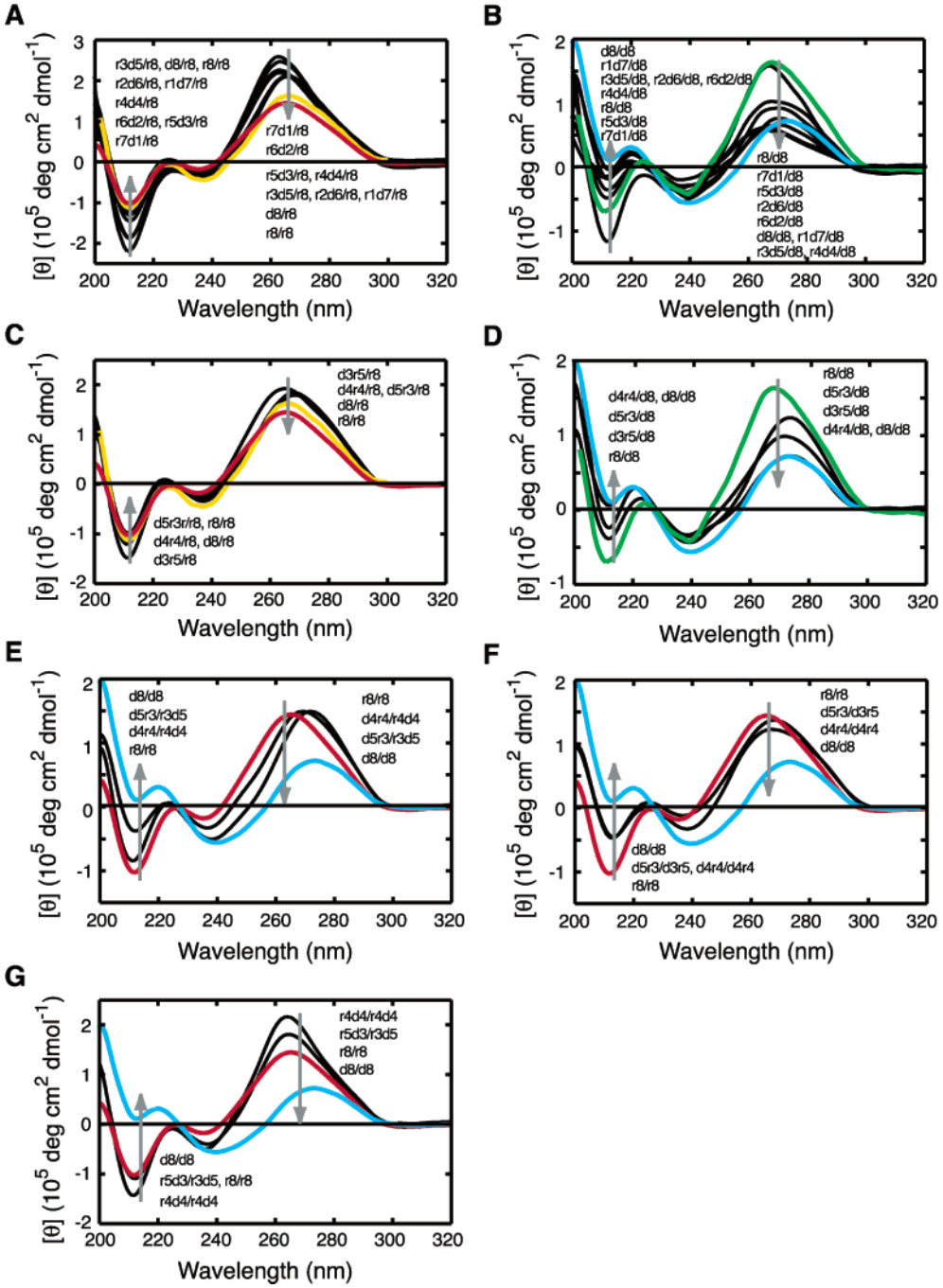

Figure 2. CD spectra of the (A) RNA−DNA/RNA, (B) RNA−DNA/DNA, (C) DNA−RNA/RNA, (D) DNA−RNA/DNA, (E) DNA−RNA/RNA−DNA, (F) DNA−RNA/DNA−RNA, and (G) RNA−DNA/RNA−DNA duplexes compared to the control duplexes (red: **r8/r8**, blue: **d8/d8**, green: **r8/d8**, yellow: **d8/r8**). The abbreviations are listed in Tables 1−3.

from the larger stability of the RNA/RNA interactions than the RNA/DNA ones and the similar stability of RNA/DNA to DNA/DNA.

Table 3 lists the parameters for the duplexes formed by two chimeric strands. Not only the duplex stability but also the enthalpy and entropy changes were comparable to other types of duplexes. The duplex stabilities of **r4d4/r8**, **d4r4/r8**, and **d4r4/r4d4** (−9.19, −9.41, and −8.40 kcal mol^{-1}, respectively) were greater than those of **r4d4/d8**, **d4r4/d8**, **d4r4/d4r4**, and **r4d4/r4d4** (−8.03∼−6.69 kcal mol^{-1}). Because **r4d4/r8**, **d4r4/r8**, and **d4r4/r4d4** have four RNA−RNA base pairs, whereas **r4d4/d8**, **d4r4/d8**, **d4r4/d4r4**, and **r4d4/r4d4** do not, the duplex stability may reflect the strength of the base pairs that the duplex possesses.

The duplexes in Tables 1-3 presented a wide range of stability, −11.3∼−6.5 kcal mol^{-1} in $\Delta G°_{37}$. These are convenient for investigating the thermodynamics-structure relationships of nucleic acid duplexes because they have an identical sequence, so that any changes in the CD spectrum are attributed to a change in the conformation. The free energy changes at 5 °C ($\Delta G°_5$) were calculated from Tables 1−3 and plotted against the peak intensities of the CD spectra. Because the band intensity is influenced by a small uncertainty of the nucleotide concentra-

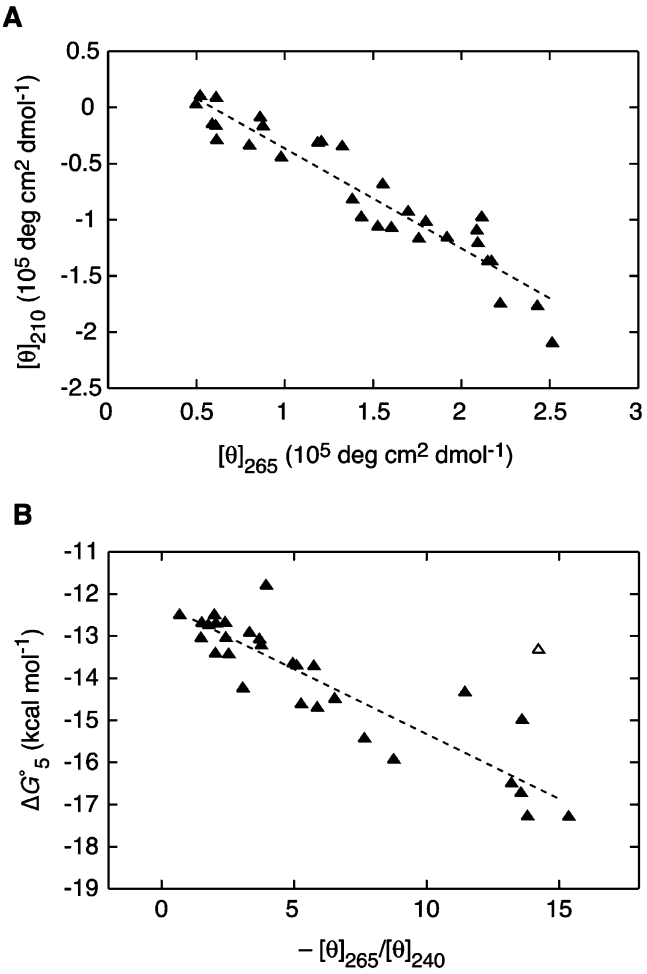

Figure 3. (A) Plot of the CD intensities at 210 nm vs those at 265 nm of the duplexes in Tables 1−3. The linear least-squares fit is indicated (a linear-correlation coefficient $r = 0.95$). (B) Plot of $\Delta G°$ at 5 °C vs the ratio of the CD intensity at 265 nm with that at 240 nm. The open symbol indicates the data containing a large uncertainty because of a small absolute value of $[\theta]_{240}$ ($>-0.1 \times 10^5$ mdeg cm^2 dmol^{-1}). The linear least-squares fit for the closed symbols is indicated ($r = 0.90$).

tion,[17] the ratio of the intensities was also examined. Plots of the negative bands at 210 and 240 nm, and a positive band at 265 nm presented a weak relationship with $\Delta G°_5$ (data not shown),[17] and the ratio of the peak intensity at 265 nm with that at 240 nm demonstrated a clearer relationship in which the more stable duplexes showed a larger ratio (Figure 3B). Generally, the ratio of these peak intensities of an A-form duplex is greater than that of a B-form duplex. Therefore, this relationship indicates a trend that a stable duplex tends to adopt an A-like conformation, and an unstable duplex forms a B-like helix.[18] A similar observation has been suggested for G/U and G/T single mismatches in oligomer RNA/DNA hybrid duplexes.[19] These results are consistent with the observations for polymer duplexes that the thermal stability of an RNA duplex is generally greater than that of a DNA duplex when their sequences are identical.[2a−e] It should be noted that the relationships in Figure 3 were achieved based on investigations using the duplexes with the same sequence.

Evaluation of the Energy for Base Pairing at the Chimeric Junction. Although the chimeric duplexes have a junction that covalently connects a ribonucleotide and a deoxyribonucleotide, they exclusively form Watson−Crick base pairs of the RNA/RNA, DNA/DNA, or RNA/DNA. To evaluate the thermodynamic parameters for the base pair formations at the chimeric junction, the nearest-neighbor $\Delta G°_{37}$s at the junctions were calculated by subtracting the nearest-neighbor free energies of the RNA/RNA, DNA/DNA, and RNA/DNA in a duplex from the observed $\Delta G°_{37}$. Because the initiation factor for the chimeric duplexes was unknown, we applied a theoretically determined free energy of 3.4 kcal mol^{-1} [20] to compare with the parameters of RNA/RNA, DNA/DNA, and RNA/DNA. The $\Delta G°_{37}$s for the junction formation calculated from the data in Tables 1−3 are summarized in Table 4. The table also lists two nearest-neighbor parameter sets for RNA/RNA,[11b,g] two parameter sets for DNA/DNA,[11e,f] and one parameter set for RNA/DNA and DNA/RNA.[3] The values of the parameters are inherently influenced by the value of the initiation factor, so that the nearest-neighbor parameter becomes more negative when a larger initiation value is applied.

Although each parameter for the chimeric junction was determined from a single sequence, they are valuable for a comparison with those of RNA/RNA, DNA/DNA, RNA/DNA, and DNA/RNA. The $\Delta G°_{37}$s at the RNA−DNA/RNA junction (rd/rr) are −2.8, −3.2, −1.8, −1.4, −2.0, −2.2, and −2.7 kcal mol^{-1} for rGdT/rAC, rGdG/rCC, rAdG/rCU, rUdA/rUA, rCdT/rAG, rAdC/rGU, and rGdA/rUC, respectively, in which rGdG/rCC is the most stable nearest-neighbor set, although rUdA/rUA is the least stable. The parameters also indicate that the chimeric junction is formed even at the helix terminus. Figure 4A compares the differences of these parameters with those of RNA/RNA (rr/rr), DNA/DNA (dd/dd), and RNA/DNA (dd/rr and rr/dd). Intriguingly, the parameters of rd/rr are close to those of rr/rr (−2.1, −2.9, −1.7, −1.1, −1.7, −2.1, and −2.3 kcal mol^{-1} for rGU/rAC, rGG/rCC, rAG/rCU, rUA/rUA, rCU/rAG, rAC/rGU, and rGA/rUC, respectively), but differ significantly from the other parameters. On the other hand, the parameters of the RNA−DNA/DNA junctions (rd/dd) are similar to those of rr/dd (Figure 4B). These observations imply that the chimeric junction in the RNA−DNA strand behave like an RNA strand and that of the DNA−RNA strand behaves like a DNA strand, although the differences in the $\Delta G°_{37}$s determined at the terminal rGdT/rAC and rGdT/dAC are slightly larger than those determined at other positions. It should be emphasized that if the initiation factor for the chimeric duplexes is not 3.4 kcal mol^{-1} and the comparisons are also carried out with another parameter sets whose initiation factor is not 3.4 kcal mol $^{-1}$, the trends

(17) It is recognized that estimation of the nucleotide concentration includes an ~10% uncertainly. The experimental uncertainty affects the peak intensity while it does not change the shape of the spectra. This would cause a weak correlation between the peak intensity and the stability. To eliminate the uncertainty in the concentration, we used the ratio of the peak intensity at 265 nm with that at 240 nm as shown in Figure 3B. A plot of the ratio of the peak intensity at 270 nm with that at 240 nm also showed a linear fit with a linear-correlation coefficient (r) of 0.89 (data not shown).

(18) Generally, the CD spectrum of a duplex is unaffected by the ionic concentration at a temperature below T_m, whereas the stability decreased at lower ionic conditions. Because a linear free energy relationship is found for $\Delta G°_{37}$s at 1 M NaCl with those at 100 mM NaCl [Nakano, S.; Hara, H.; Sugimoto, N. *Nucleic Acids Res.* **1999**, *27*, 2957.], the relationship may also be observed at lower ionic conditions.

(19) Sugimoto, N.; Nakano, M.; Nakano, S. *Biochemistry* **2000**, *39*, 11 270.

(20) On the basis of the approximate number of available conformations for the bonds in a nucleotide chain, propagation of a helix is associated with the propagation conformational entropy change ($\Delta S°$) of −11 cal mol^{-1}K^{-1}, leading to an unfavorable component of 3.4 kcal mol^{-1} in $\Delta G°$ at 37 °C.[1]

Table 4. Comparison of the Nearest-Neighbor $\Delta G°_{37}$ (kcal/mol)[a]

NN sets	rd/rr	rd/dd	dr/rr	dr/dd	dr/rd	dr/dr	rd/rd	rr/rr[b]		dd/dd [c]		rr/dd [d]	dd/rr [d]
GU/AC	−2.8	−2.1						−2.1	−2.24	−1.5	−1.44	−1.1	−2.1
GG/CC	−3.2	−2.6						−2.9	−3.26	−2.1	−1.84	−2.9	−2.1
AG/CU	−1.8	−2.2	−2.0	−1.3	−0.7	−1.7	−2.5	−1.7	−2.08	−1.5	−1.28	−1.8	−0.9
UA/UA	−1.4	−0.7	−1.7	−0.7	−0.6	−0.9	−2.0	−1.1	−1.33	−0.9	−0.58	−0.6	−0.6
CU/AG	−2.0	−0.9	−3.2	−1.8				−1.7	−2.08	−1.5	−1.28	−0.9	−1.8
AC/GU	−2.2	−1.9						−2.1	−2.24	−1.5	−1.44	−2.1	−1.1
GA/UC	−2.7	−1.2						−2.3	−2.35	−1.5	−1.30	−1.3	−1.5
CG/CG	−1.7	−2.0					−1.7	−2.0	−2.36	−2.8	−2.17	−1.7	−1.7
GC/GC	−3.3	−2.2						−3.4	−3.42	−2.3	−2.24	−2.7	−2.7
initiation[e]	3.4	3.4	3.4	3.4	3.4	3.4	3.4	3.4	4.09	3.4	1.96	3.1	3.1

[a] The notation in each column is the same alignment as the nearest-neighbor (NN) sets where r and d indicate the ribonucleotide and deoxyribonucleotide, respectively. The nearest-neighbor base sets denoted as U in the ribonucleotides are replaced by T in the deoxyribonucleotides. The parameters were calculated based on the nearest-neighbor model with the assumption that the initiation factor is 3.4 kcal mol^{-1}. The error in the parameters was estimated to be <0.3 kcal mol^{-1}. [b] From the reports by Freier et al.[11b] (left column) and by Xia et al.[11g] (right column). [c] From the reports by Sugimoto et al.[11e] (left column) and by SantaLucia Jr.[11f] (right column). [d] From the report by Sugimoto et al.[3] [e] The initiation parameters are the values for the G/C base pair formation.

described herein still hold, as is indicated by the small fluctuations of the plots for the closed symbols in Figures 4A and 4B.

We then carried out the prediction of the thermodynamic parameters in Table 1 with the nearest-neighbor parameters of rr/rr or rr/dd in place of those of rd/rr or rd/dd, respectively. The predictions indicated in the parentheses in Table 1 are close to the observed values with average differences of 3.7% in $\Delta G°_{37}$ and 1.6 °C in T_m, comparable to the errors reported for the predictions of RNA/RNA, DNA/DNA, and RNA/DNA duplexes.[3,11e−g] The predictions of $\Delta H°$ and $\Delta S°$ for the RNA−DNA/RNA duplexes were also in good agreement with the experimental values, whereas the predictions for the RNA−DNA/DNA duplexes provided somewhat larger differences as was also observed for **d8/d8**.

Figure 4C indicates that the stabilities of dr/dd and dr/dr are close to those of dd/dd, and those of dr/rd are similar to those of dd/rr. Again, the chimeric junction in the DNA−RNA strand behaves like a DNA strand and that in the RNA−DNA strand behaves like an RNA strand. In other words, the 5′-nucleotide is crucial for the stability of the chimeric junction. The predictions of the thermodynamic parameters were also successful with the nearest-neighbor parameters for RNA/RNA, DNA/DNA, and RNA/DNA duplexes (Tables 2 and 3). In contrast, those of the DNA−RNA/RNA and RNA−DNA/RNA−DNA duplexes deviated from the assumption that the RNA−DNA strand behaves like an RNA strand and that the DNA−RNA strand behaves like a DNA strand. The differences in $\Delta G°_{37}$ between dArG/rCU and dAG/rCU, dTrA/rUA and dTA/rUA, and dCrU/rAG and dCT/rAG are 1.1, 1.1, and 1.4 kcal mol^{-1}, respectively, and those between rAdG/rCdT and rAG/rCU, and rUdA/rUdA and rUA/rUA are 0.8 and 0.9 kcal mol^{-1}, respectively. The junction-independent stabilization by ∼1 kcal mol^{-1} may be a contribution from the helix initiation factor.

Thermodynamic Parameters for the Self-Complementary Chimeric Duplexes. Previously, we reported CD spectra and the thermodynamic parameters for the alternating CG sequence of r(CGCGCG) (**r6**), r(CGCGC)d(G) (**r5d1**), r(CGCG)d(CG) (**r4d2**), r(CGC)d(GCG) (**r3d3**), r(CG)d(CGCG) (**r2d4**), r(C)d(GCGCG) (**r1d5**), and d(CGCGCG) (**d6**) forming a self-complementary duplex.[21] Measurements of their thermodynamic parameters (see Supporting Information) revealed that the duplexes of **r3d3** and **r2d4** were the least stable, and the duplex of **r6** was the most stable among the duplexes. Table 4 also includes the nearest-neighbor parameters obtained from these data. The stabilities at the chimeric junction of rCdG/rCG (−1.7 kcal mol^{-1}) and rGdC/rGC (−3.3 kcal mol^{-1}) are similar to those of rCG/rCG (−2.0 kcal mol^{-1}) and rGC/rGC (−3.4 kcal mol^{-1}), respectively. Also, those of rCdG/dCG (−2.0 kcal mol^{-1}) and rGdC/dGC (−2.2 kcal mol^{-1}) are close to those of rCG/dCG (−1.7 kcal mol^{-1}) and rGC/dGC (−2.7 kcal mol^{-1}), respectively. The analysis for the self-complementary chimeric duplexes also supports the model that a 5′-side nucleotide at the chimeric junction primarily determines the strength of the interaction. In addition, the stability of rCdG/rCdG (−1.7 kcal mol^{-1}) is close to that of rCG/rCG (−2.0 kcal mol^{-1}), although the set of rd/rd derived from Table 3 deviates from the model. This may reflect a different thermodynamic contribution depending on the sequence and the junction such as the helix initiation factor, which remains to be addressed.

Interactions that Involve the 2′-Hydroxyl Group of Ribonucleotide. A number of three-dimensional structures have been reported for the chimeric duplexes.[22] In most cases, the overall conformation resembles an A-form, although the local geometry exhibits considerable variations. Crystal structures of the self-complementary duplexes of r(G)d(CGTATACGC),[22b] d(GCGT)r(A)d(TACGC),[22b] d(CCGGC)r(G)d(CCGG),[22c] and d(CCACTAGTG)r(G)[22f] revealed a feature that a single ribonucleotide in a DNA duplex converts the B-form to the A-form. The CD spectra in Figures 2B, 2D, and 2E indicate that most of the chimeric duplexes containing DNA Watson−Crick base pairs exhibit an A-like signal, although the spectrum of **r1d7/d8** that replaced a terminal dG by rG in **d8/d8** did not. Interestingly, the positive band at 265 nm for the RNA−DNA/DNA and DNA−RNA/DNA duplexes was smaller than that of **r8/r8**, while the spectra of the DNA−RNA/RNA−DNA duplexes were similar to **r8/r8**. The RNA/RNA interactions might induce the B-form to A-form conversion more efficiently than the RNA/DNA interactions.

It has been recognized that an A-form structure of the RNA duplex is associated with intramolecular interactions of the ribose 2′-hydroxyl groups as well as the C3′-*endo* sugar

(21) (a) Sugimoto, N.; Matsumura, A.; Sugano, T.; Sasaki, M. *Mem. Konan University Sci. Ser.* **1992**, *39*, 189. (b) Sugimoto, N.; Matsumura, A.; Katoh, M.; Sasaki, M. *Nucleic Acids Symp. Ser.* **1992**, 139.

(22) (a) Egli, M.; Usman, N.; Zhang, S. G.; Rich, A. *Proc. Natl. Acad. Sci. U.S.A.* **1992**, *89*, 534. (b) Egli, M.; Usman, N.; Rich, A. *Biochemistry* **1993**, *32*, 3221. (c) Ban, C.; Ramakrishnan, B.; Sundaralingam, M. *J. Mol. Biol.* **1994**, *236*, 275. (d) Salazar, M.; Fedoroff, O. Y.; Reid, B. R. *Biochemistry* **1996**, *35*, 8126. (e) Hsu, S. T.; Chou, M. T.; Cheng, J. W. *Nucleic Acids Res.* **2000**, *28*, 1322.

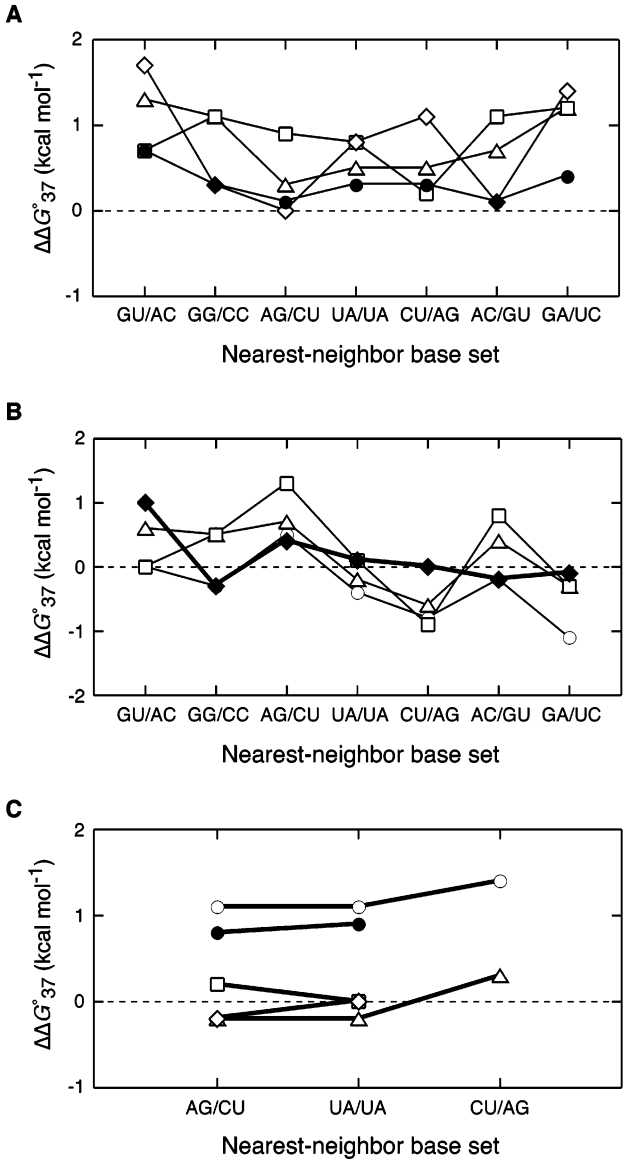

Figure 4. (A) Difference in the nearest-neighbor $\Delta G°_{37}$ values ($\Delta\Delta G°_{37}$) between rd/rr and rr/rr (circles), dd/dd (triangles), rr/dd (diamonds), or dd/rr (squares). The average values of $\Delta\Delta G°_{37}$ are 0.31, 0.80, 0.77, and 0.86, respectively. The closed symbols indicate the comparison on the basis of a model that the chimeric junction in the DNA−RNA strand behaves like a DNA strand and the RNA−DNA strand behaves like an RNA strand. The nearest-neighbor base sets denoted as U in the ribonucleotides are replaced by T in the deoxyribonucleotides. (B) The $\Delta\Delta G°_{37}$ values between rd/dd and rr/rr (circles), dd/dd (triangles), rr/dd (diamonds), or dd/rr (squares). The average values of $\Delta\Delta G°_{37}$ are −0.33, 0.16, 0.13, and 0.21, respectively. (C) The $\Delta\Delta G°_{37}$ values for dr/rr (open circles), dr/dd (triangles), dr/rd (diamonds), dr/dr (squares), and rd/rd (closed circles) subtracted by the nearest-neighbor parameter sets of dd/rr, dd/dd, dd/rr, dd/dd, and rr/rr, respectively. The average values of $\Delta\Delta G°_{37}$ are 1.2, 0.03, −0.10, 0.10, and 0.85, respectively.

puckering which is preferred by the hydroxyl group.[1] A number of interactions involving the 2′-hydroxyl group of RNA are found not only through the hydrogen bonds with phosphate oxygen atoms, O4′ of the 3′-adjacent ribose, and bases, but also through the water-mediated hydrogen bonds with the phosphates and the bases.[22a,b,23] Molecular dynamics simulations suggest the 2′-OH of the C3′-*endo* ribose puckers orientating favorably to the O3′ of the same sugar and the formation of a hydrogen bond between the 2′-H (C2′−H2′) and the O4′ of a 3′-neighboring nucleotide, which was also supported by analysis of the crystallographic structures of the A-form duplexes.[24] The thermodynamic contributions of the intra-strand hydrogen bonds may also contribute to the stability of the duplexes that include PNA (peptide nucleic acid) strands[25] which have potential intra-strand hydrogen bond sites at the backbone. The molecular dynamics simulations also indicate that the water molecules linked to the 2′-hydroxyl groups can be located over the O3′ and O4′ atoms of the same residue and the base atoms.[24] These interactions involving the 2′-hydroxyl group directly or indirectly are located in the atoms of a 3′-neighboring nucleotide or the same residue. In addition, the solution structure of a self-complementary duplex of d(CGC)r(AAA)d(TTTGCG) revealed that the structural parameters of the cytosine at the DNA-RNA junction were not affected by the 3′-ribonucleotides, while those of the thymine at the RNA−DNA junction were changed by the 5′-ribonucleotides.[22e] This observation suggests that the 5′-ribose may influence the conformation of the 3′-neighboring nucleotide, consistent with our observation that the 5′-nucleotide at the chimeric junction affects the strength of the interaction. We therefore propose that the nearest-neighbor interaction involves the contribution of the 2′-hydroxyl group as well as the hydrogen bonds in base pairing and stacking interactions between adjacent base pairs. The 2′-hydroxyl group would affect the cation and the hydration network around the helix, which may also be associated with the nearest-neighbor interaction.

It is reported that whether the 2′-hydroxyl group stabilizes or destabilizes a duplex differs depending on the type of DNA/DNA, RNA/RNA, and RNA/DNA duplex.[2f,19] Here, duplex destabilization and stabilization by substitution of a ribonucleotide for a deoxyribonucleotide were observed, and we found that this observation could be interpreted by considering the strength of the nearest-neighbor interaction before and after the substitution. There are 100 kinds of possible nearest-neighbor base sets for the chimeric junctions. Determination of these thermodynamic parameters is a time-consuming task. Alternatively, we addressed the prediction without extensive efforts. Importantly, a comparison with the parameters for other types of duplexes addressed the roles of ribose in the duplex stability. Understanding the influences of ribonucleotide would be also useful for the design of artificial nucleotides that strongly bind to nucleotides.

Acknowledgment. This work was supported in part by Grants-in-Aid for Scientific Research from the Ministry of Education, Science, Sports and Culture, Japan.

Supporting Information Available: The parameters for the self-complementary duplexes of an alternating CG sequence, and the melting curves of the duplexes in Tables 1−3 (PDF). This material is available free of charge via the Internet at http://pubs.acs.org.

JA037314H

(23) Hsu, S. T.; Chou, M. T.; Chou, S. H.; Huang, W. C.; Cheng, J. W. *J. Mol. Biol.* **2000**, *295*, 1129.
(24) Auffinger, P.; Westhof, E. *J. Mol. Biol.* **1997**, *274*, 54.
(25) Sugimoto, N.; Satoh, N.; Yasuda, K.; Nakano, S. *Biochemistry* **2001**, *40*, 8444.